JOURNAL OF GEOPHYSICAL RESEARCH, VOL. 105, NO. B2, PAGES 2903–2914, FEBRUARY 10, 2000

Helium diffusion from apatite: General behavior as illustrated by Durango fluorapatite

K. A. Farley

Division of Geological and Planetary Sciences, California Institute of Technology, Pasadena

Abstract. High-precision stepped-heating experiments were performed to better characterize helium diffusion from apatite using Durango fluorapatite as a model system. At temperatures below 265°C, helium diffusion from this apatite is a simple, thermally activated process that is independent of the cumulative fraction of helium released and also of the heating schedule used. Across a factor of ~4 in grain size, helium diffusivity scales with the inverse square of grain radius, implying that the physical grain is the diffusion domain. Measurements on crystallographically oriented thick sections indicate that helium diffusivity in Durango apatite is nearly isotropic. The best estimate of the activation energy for He diffusion from this apatite is E_a = 33 ± 0.5 kcal/mol, with $\log(D_0)$ = 1.5 ± 0.6 cm^2/s. The implied He closure temperature for a grain of 100 μm radius is 68°C assuming a 10°C/Myr cooling rate; this figure varies by ±5°C for grains ranging from 50 to 150 μm radius. When this apatite is heated to temperatures from 265 to 400°C, a progressive and irreversible change in He diffusion behavior occurs: Both the activation energy and frequency factor are reduced. This transition in behavior coincides closely with progressive annealing of radiation damage in Durango apatite, suggesting that defects and defect annealing play a role in the diffusivity of helium through apatite.

1. Introduction

Several recent studies have documented helium diffusion in uranium- and thorium-rich minerals such as apatite to evaluate and calibrate the (U-Th)/He dating technique for thermochronometry [*Zeitler et al.*, 1987; *Lippolt et al.*, 1994; *Wolf et al.*, 1996b; *Warnock et al.*, 1997; *Reiners and Farley*, 1999]. In-vacuum He diffusion measurements suggest that (U-Th)/He ages of apatite record cooling through lower temperatures than other dating techniques, and apatite He ages from a variety of settings provide evidence of the applicability and potential value of this new technique [e.g., *Wolf et al.*, 1996a; *House et al.*, 1998]. However, important questions remain regarding the behavior of He diffusion from apatite, justifying this detailed laboratory study.

A precise and accurate knowledge of the diffusion behavior of a radiogenic daughter product is required to establish the temperature range over which a particular dating technique is sensitive. In the simplest case, the radiogenic daughter product would be lost by volume diffusion involving a single, thermally activated process for all of the daughter in the crystal. Under such conditions the temperature dependence of diffusivity is characterized by an activation energy (E_a) and diffusivity at infinite temperature (D_0): $D/a^2 = D_0/a^2 \exp(-E_a/RT)$, where R is the gas constant, T is the temperature, and a is the diffusion domain radius. Laboratory measurements of diffusivity over a range of temperatures will in this case yield a line on an Arrhenius plot with slope proportional to E_a and y intercept of $\ln(D_0/a^2)$. From these two quantities a closure temperature can be computed [*Dodson*, 1973], or, more generally, ages can be calculated numerically along arbitrary time-temperature paths. Provided diffusion in the natural setting behaves identically to that in a vacuum chamber, these measurements are sufficient to interpret an apparent age but only for the characterized sample. For more general application it would be valuable to know how variable E_a and D_0 are and what physico-chemical factors, if any, control them. Similarly, it is important to determine the physical significance of the diffusion domain size a. In some cases of noble gas diffusion from minerals the domain is the crystal itself [*Reiners and Farley*, 1999], while in others it is a subgrain structure that may be highly variable in size both within and between crystals [*Lovera et al.*, 1991].

Previous studies suggest that volume diffusion is the dominant mechanism by which He is released from apatite. On an Arrhenius plot, He diffusion from all apatites so far investigated displays the same basic pattern: a linear regime at low temperatures that deviates from linearity toward lower diffusivities at temperatures above about 300°C [*Zeitler et al.*, 1987; *Lippolt et al.*, 1994; *Wolf et al.*, 1996b; *Warnock et al.*, 1997]. The origin of this transition in behavior is not yet understood. Because no helium is retained over geologic timescales at temperatures above 300°C, *Wolf et al.* [1996b] argued that this high-temperature behavior is irrelevant to thermochronometric applications. However, it is possible that this observation signals complex behavior occurring even at temperatures <300°C. Considering only the low-temperature regime reveals consistently linear Arrhenius behavior for He diffusivity, with little variability in diffusion parameters among the specimens thus far investigated. For example, the variation in activation energy in the samples studied by *Wolf et al.* [1996b] is 30 to 39 kcal/mol, with most ~35 kcal/mol. It is unclear whether this variability is real or reflects analytical errors; there is no strong evidence that diffusivity is related to apatite chemical composition. Similarly, there is no obvious systematic behavior in D_0/a^2 among reported results. On the basis of the absence of detectable variation in D_0/a^2 among specimens that varied in grain size and shape, *Wolf et al.* [1996b] concluded that the He

Copyright 2000 by the American Geophysical Union.

Paper number 1999JB900348.
0148-0227/00/1999JB900348$09.00

diffusion domain in apatite is smaller than the crystal itself. Taken together, these observations suggest a He closure temperature of ~75°C for most apatites. There is no indication from existing data whether helium diffusion is isotropic, but diffusion of some other substances in apatite is strongly anisotropic [*Farver and Giletti*, 1989].

This paper presents new high-precision He diffusion data on Durango apatite. This large gem-quality apatite provides an ideal model system for detailed characterization of He diffusion behavior. The experiments described here confirm most aspects of previous studies, such as the existence of strongly Arrehenian behavior below ~300°C and an implied closure temperature near 75°C. However, several previous observations on Durango (and other) apatites are not. In particular, the new data indicate that the diffusion domain is the grain itself; thus contrary to previous work, the closure temperature varies with grain size. In addition, the data demonstrate that irreversible changes in He diffusion behavior occur when Durango apatite is heated above ~265°C. These observations have important implications for the interpretation of He diffusion data and for apatite He ages. K. A. Farley (manuscript in preparation, 2000) describes results of similar high-precision diffusion experiments performed on more typical apatite samples.

2. Sample and Methods

A variety of experiments were performed on gem-quality crystals of fluorapatite from Cerro de Mercado, Durango, Mexico [*Young et al.*, 1969], obtained from the California Institute of Technology (Caltech) mineral collection. On the basis of >30 determinations at Caltech this specimen has a He age of 32.1 Ma, consistent with independent estimates of the age of associated volcanics [*McDowell and Keizer*, 1977]. As a consequence of its high radioelement content (~160 ppm Th; ~9 ppm U) and moderate age, this apatite has a relatively high He content, 8.7 nmol/g. Experiments were performed both on grain fragments wet-sieved to various sizes and on thick sections (150–250 μm thick) cut either parallel or perpendicular to the c axis of the crystal. All aliquots of grain fragments were from a single large crystal from which a >50-μm-thick surface layer was cut to eliminate the effects of α ejection [*Farley et al.*, 1996]. The grain fragments tend to be angular and elongated shards, so sieving does not yield a tight grain size distribution. The thick sections were all obtained from the interior of a second gem-quality crystal.

Stepped-heating experiments were performed on a few milligrams of apatite wrapped in copper foil and suspended from a thermocouple wire in a small vacuum chamber. This package was heated by radiation from a light bulb projected through a sapphire window. The thermal response characteristics of this apparatus [*Farley et al.*, 1999] and its use for He diffusion studies from titanite [*Reiners and Farley*, 1999] have been described elsewhere. This apparatus has the advantage that temperature is measured within just a few millimeters of the sample; given the high conductivity of the copper foil envelope, the thermocouple likely indicates the sample temperature fairly accurately. For most experiments a T-type thermocouple with special limits of error (supplied by Omega Engineering) was used because it gives the highest available precision for temperatures lower than 350°C. At higher temperatures a K-type thermocouple was used. Temperature was regulated by varying the power supplied to the bulb using a Watlow 945 proportional temperature controller. Estimated precision and accuracy of the temperature measurements is about ± 2°C (2σ); this uncertainty figure is supported by reproducibility of diffusion experiments presented below. Compared to the previous apparatus used at Caltech [*Wolf et al.*, 1996b], the present device provides better temperature accuracy and far more rapid thermal response.

Helium was extracted from the apatites and accumulated in the chamber for periods ranging from 15 min to several weeks. The evolved helium was spiked with ~0.5 pmol of 99.3% pure ^{3}He and measured on a Balzers Prisma quadrupole mass spectrometer after cryogenic concentration and purification. The amount of spike delivered was repeatedly cross-calibrated against a pipette that delivers a known amount of ^{4}He determined to high precision and accuracy with a capacitance manometer. On the basis of reproducibility of standards the precision of He determinations presented here is better than 1% down to a few times the blank level. Blanks were essentially invariant with both time and temperature in the diffusion cell and were typically <1 fmol. All plotted data have been blank corrected; in general, the blank corrections are small (<2%), but in rare cases, blank correction is a substantial fraction of the total gas in a step. When blank corrections for a given data point exceeded 35% the point was ignored for plotting and interpretation.

Experiments on single apatite aliquots involved a few to more than 100 individual steps. Temperature-cycling experiments were used extensively to investigate whether complex heating schedules would yield results distinct from those obtained previously using only monotonically increasing temperature steps. Integrated gas yields from the incremental outgassing experiments ranged from a few percent to nearly 100% of the total in the sample. In all cases the final step was fusion in a double-walled vacuum furnace to ensure complete He extraction. Diffusion coefficients were computed from fractional gas yield and holding time assuming spherical diffusion geometry [*Fechtig and Kalbitzer*, 1966], except where noted otherwise. As discussed below, this assumption is not strictly correct, but assumption of a different geometry would not substantially affect the results or their interpretation.

3. Results

Results of the diffusion experiments are presented as Arrhenius plots in the figures and as calculated diffusion parameters in Table 1. (A full data table is available upon request from the author.)

3.1. Temperature Cycling (<300°C) and Grain Size Effects

Figure 1 presents results of two experiments performed on aliquots of 160–180 μm grain fragments, identical to those used in previous studies of Durango apatite [*Zeitler et al.*, 1987; *Wolf et al.*, 1996b]. In the first experiment the aliquot was heated monotonically from 120 to 300°C in 50 steps (see Figure 1, bottom, for heating schedule). This schedule released 24% of the helium in the sample. In the second experiment, essentially the same temperature range was investigated, but temperatures initially decreased, then increased, then decreased and increased again. In early experiments it was found that anomalously high diffusivities are measured immediately following a rapid and large drop in temperature during cycled runs. This effect is documented more fully in section 3.3. For the experiments described in this section the temperature schedules involved only gradually decreasing temperatures (usually 10°C per step) to avoid this complication. The final yield from this aliquot was 42%. As shown in Figure 1, the two heating schedules yield diffusivity arrays that are highly linear

Table 1. Results of Diffusivity Measurements

Experiment	Sample	$\ln(D_0/a^2)$	$\pm 2\sigma$	E_a, kcal/mol	$\pm 2\sigma$	T_c,* °C	r^2
Shards 160–180 μm	monotonic cycled	13.97	0.22	33.38	0.23	72	0.9994
		12.90	0.37	32.48	0.58	70	0.9965
Sieved shards	44–53 μm	20.16	0.18	36.72	1.82	64	0.9921
	60–74 μm	17.67	0.13	35.24	1.25	66	0.9959
	74–100 μm	18.16	0.19	36.49	1.78	75	0.9906
	100–149 μm	14.02	0.13	33.01	0.96	68	0.9955
High-temperature regime 160–180 μm shards	no preheat, segment 1†	15.07	0.13	34.60	0.47	NA	0.9994
	no preheat, segment 2†	11.27	0.08	29.80	0.29	NA	0.9996
	no preheat, segment 3†	9.76	0.22	28.30	0.79	NA	0.9980
	preheated to 360°C†	10.75	0.41	29.20	0.61	NA	0.9960
Resurfaced slabs 150 μm thick (uses slab geometry)	c perpendicular slab	13.26	0.05	32.80	0.25	71	0.9997
	c parallel slab	10.44	0.08	30.61	0.54	68	0.9992

NA, not applicable.
*Closure temperature assuming cooling rate of 10°C/Myr.
†Defined in text.

($r^2 > 0.996$) and indistinguishable from each other. There is no indication that heating schedule affects helium diffusivity in these runs. The activation energy implied by these data is 32.9 kcal/mol, and $\ln(D_0/a^2) = 13.4\ s^{-1}$. These results are similar to those reported by *Wolf et al.* [1996b] (Figure 1) but have slightly lower activation energy. In the following discussion the combined data sets for these two 160–180 μm fractions are used as a reference against which diffusivity from other experiments is compared.

To identify any relationship between grain size and diffusivity, fragments sieved into 44–53, 60–74, 74–100, and 100–149 μm fractions were analyzed at temperatures between 170 and 210°C. The heating schedule for all five of these experiments involved a cycle from low to high temperatures and back to low temperatures. Total gas yields ranged from 2% to 6%. In the smallest fractions the first few temperature steps yielded anomalously low diffusivity, possibly as a result of loss of loosely bound helium during sample processing (probably grinding); anomalous diffusivity in the first few steps is discussed more fully in section 3.2. Ignoring these few data points, He diffusivity again plots on highly linear arrays (Figure 2), with activation energies similar to those found for the large grain size fractions: 33 to 37 kcal/mol. In none of these runs is there an analytically significant difference in diffusivity between the temperature-increasing and temperature-decreasing segments of the heating schedule. However, there is a clear correspondence between diffusivity and grain size: the diffusion arrays shift upward with finer grain size. This tendency is consistent with a relationship between the physical grain size and the diffusion domain size.

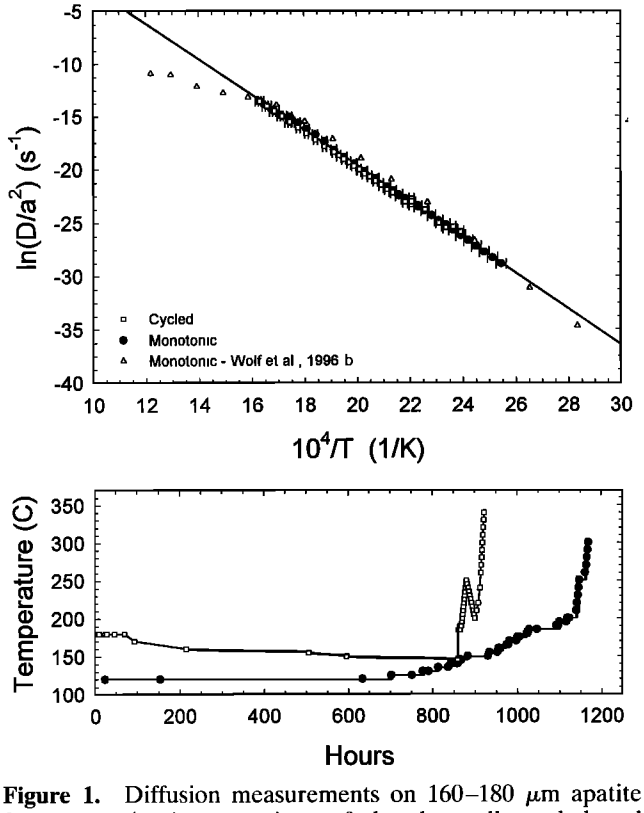

Figure 1. Diffusion measurements on 160–180 μm apatite fragments. (top) comparison of the thermally cycled and monotonic runs with each other and with the data of *Wolf et al.* [1996b] on the same sample. (bottom) Heating schedule for the two new runs.

The data in Figure 2 can be used to quantitatively test the hypothesis that the physical grain dimension is equivalent to the diffusion domain (a in D/a^2). The most obvious approach is to multiply D_0/a^2 for each sieve fraction by the grain radius squared (R^2), and examine whether D_0 is constant among the aliquots. D_0 values calculated in this way vary over 2 orders of magnitude and are uncorrelated with grain radius and with the relative position of the diffusion arrays in Figure 2. This scatter likely arises because measurement uncertainties are amplified by projection to the y intercept. As an alternative, the vertical position of the linear array for each sieve fraction can be compared to that of the 160–180 μm reference fraction. If D/a^2 varies with R^{-2}, then it is predicted that for any given temperature that $(D/a^2)_{\text{predicted}} = (R^2_{\text{ref}}/R^2)\ (D/a^2)_{\text{ref}}$. Figure 3 is a plot of predicted versus observed relative diffusivities for these aliquots. The plotted values represent averages over all temperature steps in the range plotted in Figure 2. The major source of uncertainty in this plot is the actual grain size passed by the sieves, as well as its approximation as a sphere. Despite these uncertainties, there is a fairly good correspondence between predicted and observed relative diffusivities, suggesting that the diffusion domain corresponds to the physical grain.

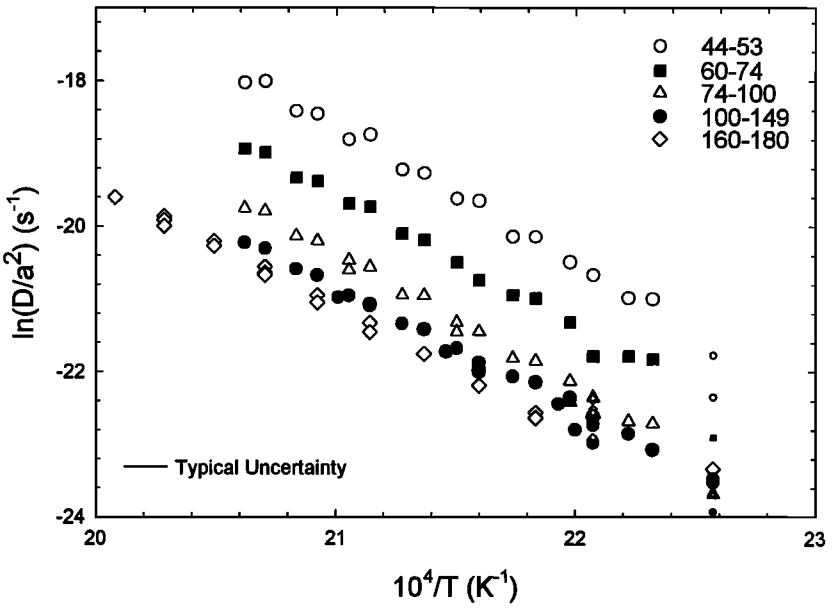

Figure 2. Diffusion measurements on sieved aliquots of Durango apatite. Sieve size ranges (in μm) are indicated for each aliquot. Data points with smaller symbols are initial steps with anomalously low diffusivity possibly arising from helium loss during sample grinding; these points have been ignored in calculation of diffusion parameters. These data show that diffusivity decreases with increasing grain size and suggest that the diffusion domain is the physical grain itself.

3.2. Crystallographically Oriented Thick Sections

To investigate whether diffusion from apatite is isotropic, several ~200-μm-thick apatite slabs were cut either perpendicular or parallel to the c axis. The slabs were typically square in section and had a length to width ratio of 10–20. Barring strong anisotropy in diffusivity, diffusion through slab faces should greatly exceed diffusion through the edges. Because the geometry in these experiments is well defined, diffusion data for these runs were computed assuming infinite slab geometry [*Crank*, 1975]. These experiments are presented in detail because they illustrate the substantial complexity that exists when measuring diffusivity from processed sections (rather

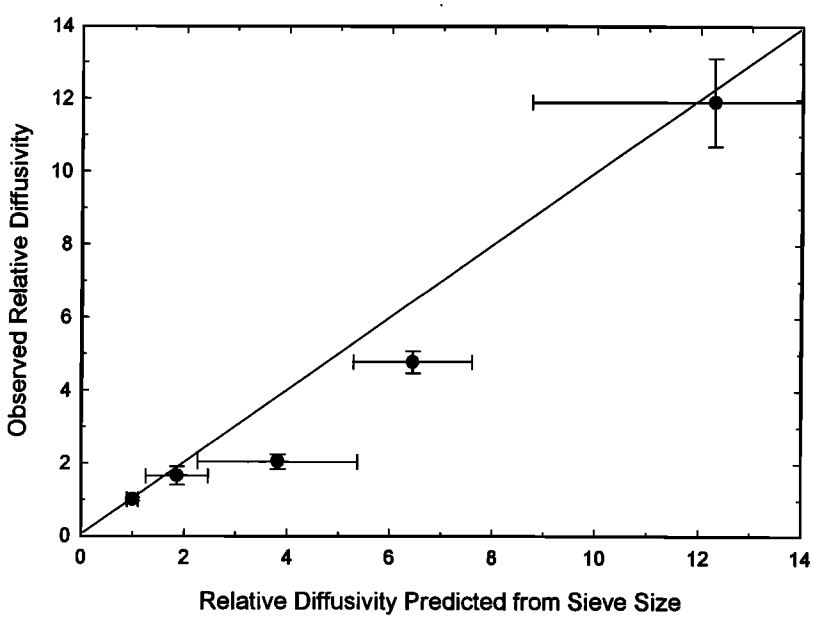

Figure 3. Comparison between observed mean diffusivity and that predicted if diffusivity scales with the inverse of the grain size squared for the data in Figure 2. Diffusivities are plotted relative to that in the 160–180 μm reference aliquots (Figure 1). The 45° line is the expected behavior if the diffusion domain is the grain itself and is a reasonable approximation of the observations. Error bars on the x axis arise from the sieving window used for each aliquot. Error bars on the y axis reflect the spread of relative diffusivity values computed from the individual temperature steps measured on each aliquot.

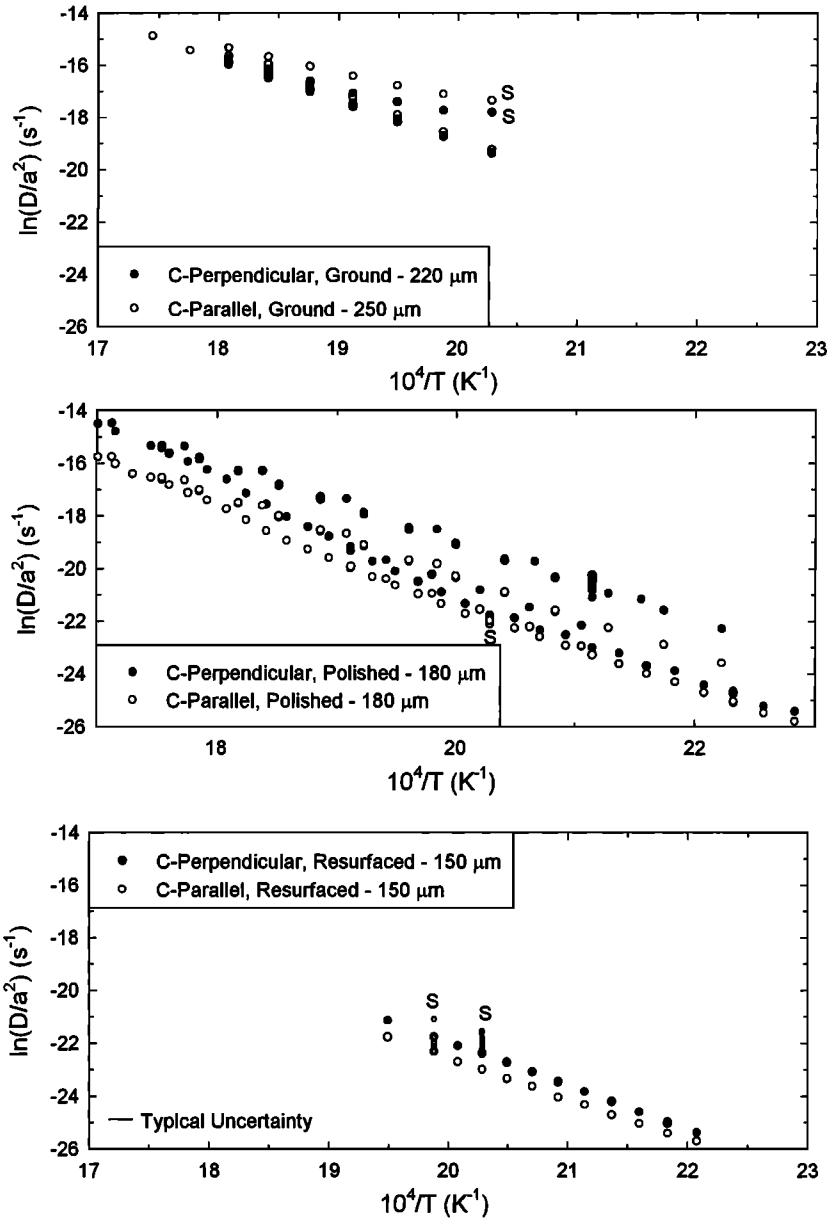

Figure 4. Helium diffusion measurements on crystallographically oriented slabs. (top) Data for the coarsely ground slabs, (middle) data for the highly polished slabs, and (bottom) data for the resurfaced slabs. In each panel, "S" indicates the diffusivity measured at the start of the experiment. The resurfaced slabs yield reasonable diffusivity arrays and indicate only a modest difference in helium diffusion in the *c* parallel and *c* perpendicular directions. In contrast, both the coarsely ground and highly polished slabs yield curved arrays. See text for details.

than whole grains or grain fragments). Three sets of experiments were performed on slabs differing only in surface treatment: (1) "coarsely ground," for which slabs were cut and ground to the desired thickness with coarse (30 μm) alumina grit, (2) "highly polished," for which slabs were cut, ground, and polished following traditional thin-sectioning procedures involving a high-speed lap wheel; the final step was polishing with 0.1 μm grit, and (3) "resurfaced," for which to investigate possible artifacts induced by polishing, the outermost >10 μm of each face of fresh aliquots of the "highly polished" slabs were removed by hand grinding with 3-μm grit. Arrhenius plots for these experiments are shown in Figure 4. Both the *c*-parallel and *c*-perpendicular coarsely ground slabs exhibit initially shallow slopes which curve upward as the experiment proceeds. This is most apparent from a comparison of the initial steps obtained on the rising portion of the temperature schedule to later steps obtained at the same temperature on the downward portion. For example, for the *c*-perpendicular section the initial step at 220°C yielded a diffusivity 1.5 ln units higher than the value obtained at this temperature after cycling to 280°C. The magnitude of the discrepancy for the *c*-parallel slab is similar. A possible explanation for these results is that the slabs are rough enough to cause high diffusivity from small surface domains. The influence of these domains is expected to decrease during the experiment as they become increasingly depleted of helium. If this is the correct explanation, diffusivity

should ultimately fall onto a single Arrhenius array after sufficient helium is removed; this array should correspond to that for diffusion through the entire slab. Indeed, both slabs do seem to approach an array that retains its position as the experiment progresses, after ~5% of the helium has been removed. However, it is difficult to show from these data that the ultimate state has been achieved, i.e., that the surface domains have been completely depleted. In addition, it is hard to rule out other explanations for the anomalous behavior of these slabs.

To test for an affect of surface roughness on He diffusion from the coarsely ground slabs, highly polished oriented slabs of slightly smaller thickness were prepared. As shown in Figure 4, these slabs also show anomalous diffusivity, but now the diffusivity increases as the experiment proceeds. For example, the initial 220°C step yields a diffusion coefficient 1 ln unit lower than a step at the same temperature after heating to 250°C and removal of ~1% of the helium. Again the *c*-parallel slab displays a remarkably similar pattern. Furthermore, these diffusion arrays plot almost 3 ln units lower than the coarsely ground slabs. Clearly, the degree of surface polishing and grinding has a profound effect on helium diffusion from apatite. Polishing apparently thermally or mechanically modifies the crystal in such a way as to reduce the helium yields in the initial steps relative to those at the same temperature in later steps. The simplest explanation for these results is that the outermost few μm of the slab have lost helium. *Fechtig and Kalbitzer* [1966] discuss the consequences of such rounded concentration profiles on noble gas diffusion measurements.

The final set of slab experiments involved removal of the outermost ~10 μm from the surfaces of virgin aliquots of the polished sections. These "resurfaced" slabs were polished very slowly by hand to minimize thermal and mechanical damage. In addition, initial steps were isothermal to verify that a stable diffusivity was obtained before cycling the temperature. This precaution ensures that the initial surface effects have been removed and that the final Arrhenius array represents diffusion through the slab itself. The *c*-perpendicular slab yields initially decreasing diffusivities at 220°C that eventually stabilize to better than 0.007 ln units after ~2% gas yield. The *c*-parallel slab behaved similarly: after 2.1% of the gas was released at 230°C, diffusivity stabilized to better than 0.001 ln units. In both cases, highly linear Arrhenius plots were obtained from temperature cycling after the isothermal period. These data indicate only modest anisotropy in He diffusion. The activation energy is slightly higher in the *c*-perpendicular (32.8 ± 0.3 kcal/mol) than in the *c*-parallel slab (30.6 ± 0.5 kcal/mol), and these values are close to that obtained for the reference aliquots (32.9 ± 0.4 kcal/mol). D_0 calculated from D_0/a^2 and measured slab thicknesses is about 1 order of magnitude higher in the *c*-perpendicular slab (D_0 = 130 cm^2/s) than in the *c*-parallel slab (D_0 = 8 cm^2/s).

3.3. Behavior at Higher Temperatures: Deviation From Linearity and a Transient Response to Heating

The experiments described above were conducted at <275°C to avoid possible complications associated with the known deviation from linear Arrhenius behavior above 290°C. Additional high-temperature experiments were undertaken to better understand the origin and significance of this change in behavior. All of these experiments were performed on 160–180 μm apatite fragments. For direct comparisons with the behavior described above, the quantity $\Delta = \ln(D/a^2)_{\text{observed}} - \ln(D/a^2)_{\text{ref}}$ was computed at a given temperature, where $(D/a^2)_{\text{ref}}$ is the diffusivity interpolated or extrapolated from the regression line through the diffusivity data in Figure 1.

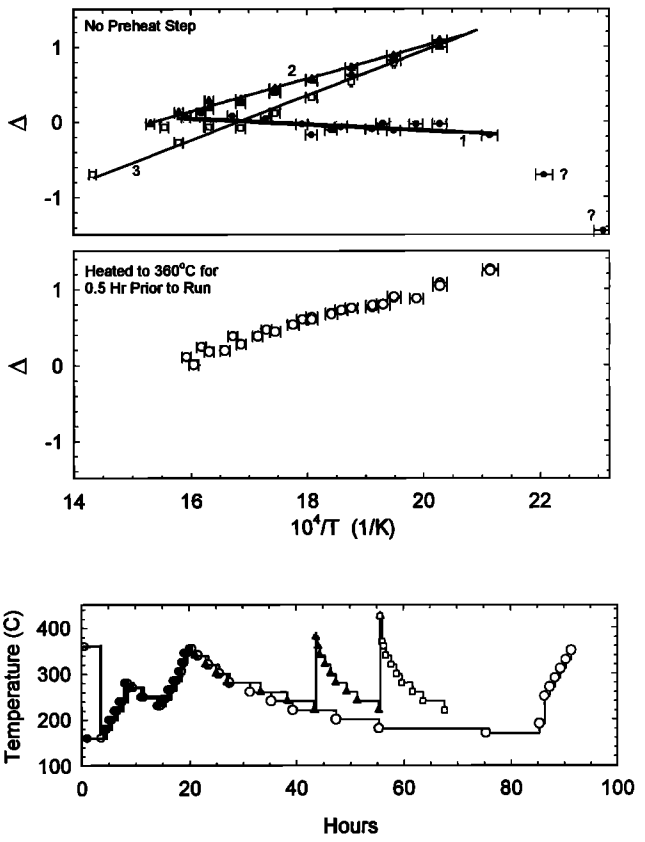

Figure 5. The irreversible effect of heating above 265°C on He diffusion from apatite. (top) and (middle) Difference between the measured diffusivity of 160–180 μm fragments and the reference aliquots (Figure 1) at the same temperature (=Δ) for two runs, one starting with no initial heating, and the other after heating to 360°C. Segments 1, 2, and 3 show progressive rotation of the diffusion array with increasing maximum temperature experienced by the sample. The 360°C aliquot is similarly rotated from the reference diffusion array (i.e., from Δ = 0). These data document an irreversible change in diffusion characteristics (toward lower E_a and D_0/a^2) that becomes progressively more pronounced as the maximum temperature experienced by the sample is increased (above 265°C). (bottom) The heating schedule for the two experiments.

In the first experiment the sample was repeatedly cycled from low to high temperature and back, with successively higher maximum temperatures with each cycle (Figure 5). The data are logically divided into three segments based on the observed diffusivity and characterized by the maximum temperature experienced by the sample before the segment was run. Segment 1, starting from room temperature, is defined by the first 16 data points. Segment 2 begins with a temperature of 355°C and includes steps 17 to 32. Segment 3 begins with a step at 425°C and is defined by steps 33 to 42. Segment 1 plots close to Δ = 0 except for the first two data points, which are low for unknown reasons. In contrast, segment 2 is linear (r^2 > 0.999) but rotated counterclockwise relative to Δ = 0, with a pivot point at the high-temperature end of the array. This implies a change to lower activation energy and frequency

factor that is retained even when the sample is cooled to low temperature. While segment 1 has E_a and $\ln(D_0/a^2)$ values of 34.6 kcal/mol and 15 s^{-1}, respectively, segment 2 has values of 29.8 kcal/mol and 11 s^{-1} (Table 1). The rotation of the third segment is even greater, implying further reduction of E_a and $\ln(D_0/a^2)$ to 28.3 kcal/mol and 10 s^{-1}, respectively.

In a second experiment the sample was subjected to a heating schedule similar to the first experiment, but only after first being heated to 360°C for 30 min. The diffusion array from this sample is also positively inclined relative to $\Delta = 0$; the array yields $E_a = 29.2$ and $\ln(D_0/a^2) = 11$ s^{-1}. These values are intermediate to those found for segments 2 and 3 in the previous experiment.

These data strongly suggest that the change in diffusion behavior is controlled by maximum temperature experienced by the sample: as the maximum temperature is increased above ~300°C, diffusion parameters change such that the array increasingly rotates counterclockwise. In contrast, the rotation of the diffusion arrays varies independently of cumulative fraction of He released.

A final set of experiments was performed to document the temperature range over which the rotation of the diffusion array occurs. These experiments involve an unusual heating schedule in which the sample is taken rapidly from high temperature (where the change in diffusivity is presumably precipitated) to low temperature (where its effects are most easily measured as high Δ values). In preliminary studies it was discovered that the first low-temperature step following a high-temperature step is often anomalously high in diffusivity compared with succeeding steps at the same temperature. This unexpected result does not arise from failure to let the sample cool sufficiently between runs, nor from inadequate pumping of the diffusion cell after the high-temperature step. Even after a sample is allowed to cool and pump for several days after a high-temperature step, diffusivity in the subsequent low-temperature step remains anomalously high. A similar transient effect after cooling has been noted in He diffusion from titanite [*Reiners and Farley*, 1999]. To document and reduce the effects of this phenomenon, the low-temperature steps were run several times in succession after each high-temperature step (Figure 6).

Figure 6 shows Δ values at 160°C measured as a function of the maximum temperature achieved by the sample and at 170°C on a second aliquot. Figure 6 clearly reveals the slowly decaying transient after each high-temperature step. Typically, diffusivity drops by ~0.2 ln units between the first and second low-temperature replicate, then falls an additional 0.1 ln unit between the second and third replicates. The magnitude of this decay is about the same each time the sample is cooled down and analyzed repeatedly at 160–170°C, with the notable exception that the effect seems to disappear after the sample has been taken to temperatures above ~400°C. Details of the decay were explored in two additional experiments after heating aliquots to 310°C and 410°C for 1 hour (details not shown). After heating to 310°C, successive diffusivity measurements at 160°C decline progressively but at an ever decreasing rate, until after 60 hours diffusivity has stabilized about 0.4 ln units lower than the first step at 160°C. After heating to 410°C, insufficient helium was released at 160°C to measure, so "low-temperature" diffusivity was measured at 210°C instead. In contrast to the results after heating to 310°C, after the 410°C step, successive low-temperature diffusivity measurements are essentially invariant.

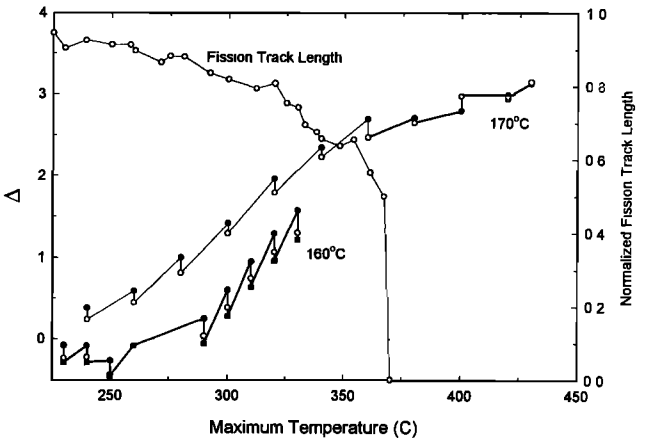

Figure 6. Progressive modification of diffusivity with maximum temperature experienced by the sample. The samples in this plot were subjected to an unusual heating schedule involving one step at a high temperature, followed by several steps at either 160°C or 170°C, followed by an even higher temperature, etc. A progressive increase in Δ (defined in caption to Figure 5) at 160–170°C occurs as the maximum temperature experienced by the sample is increased from ~265°C to ~400°C. Note also the transient elevation in diffusivity that decays away with successive steps following each high-temperature step (symbol style indicates the sequence in which each measurement was made: solid circle, first analysis; open circle, second analysis; solid square: third analysis). The transient is present in all experiments performed up to a maximum temperature of ~390°C. After this temperature the transient elevation is no longer apparent. Fission track length reduction [from *Green et al.*, 1986] occurs over the same temperature range as the change in He diffusion behavior. Track lengths are normalized to the mean length measured at temperatures <240°C.

In addition to this transient response upon cooling, the major feature apparent in Figure 6 is the onset of enhanced diffusivity (larger Δ values) that occurs after maximum temperatures of about 265°C. Below this temperature, there is no indication that Δ scales with maximum temperature, consistent with the low-temperature cycling experiments in Figure 1. However, as the maximum temperature is raised above ~265°C, Δ climbs steadily until about 390°C. Above 400°C it appears that the diffusion parameters again stabilize. Thus both the transient response and the increase of Δ values with increasing maximum temperature appear to cease above 400°C.

4. Discussion

The results of this study can be divided into two parts. The first relates to helium diffusivity at temperatures below the clear change in behavior at ~265°. It is this low-temperature behavior that is most directly relevant to helium thermochronometry [*Wolf et al.*, 1996b]. The second part relates to the complexities arising above the 265°C transition temperature. This complex behavior may or may not bear on He diffusion at the low temperatures at which helium accumulates in nature.

4.1. Low-Temperature Behavior and Implications

The most important result of this study is that helium diffusion from Durango apatite clearly obeys the behavior expected

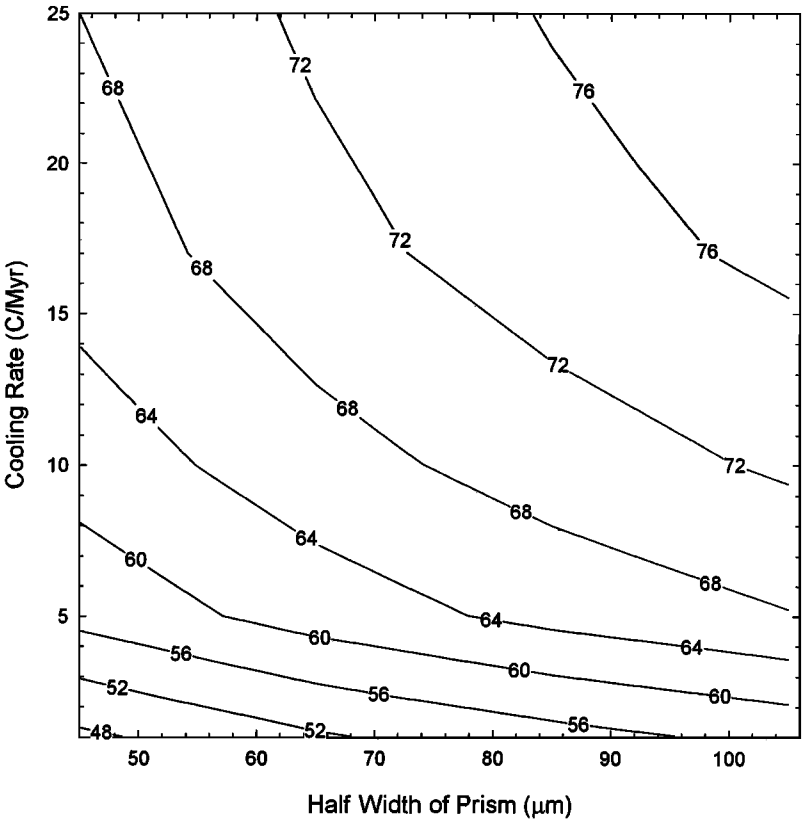

Figure 7. Helium closure temperature for apatites with Durango diffusivity characteristics as a function of apatite prism half width and cooling rate. The closure temperature was computed numerically for infinite cylinder geometry and incorporates the effects of α ejection on the He concentration profile.

for a single-mechanism thermally activated Fickian diffusion process at temperatures from ~90 to 260°C irrespective of heating schedule and fraction of helium released. On the basis of the new data in Figure 1, a best estimate for the activation energy for diffusion of He from fragments of Durango apatite is 32.9 kcal/mol ± 0.5 kcal/mol (1σ). The activation energy is nearly isotropic through the crystal: slab measurements imply an activation energy for diffusion along the c axis of 32.8 kcal/mol (derived from the slab cut perpendicular to c) and a slightly lower value of 30.6 kcal/mol for c-perpendicular diffusion. These activation energies are at the low end of previous estimates from Durango and other apatites. For example, the data of *Wolf et al.* [1996b] for Durango apatite plot on a slightly steeper array and thus yield a higher activation energy. Interestingly, the measurements of *Wolf et al.* [1996b] also have a slight concave-down curvature. The new and more precise measurements do not show curvature, suggesting a small systematic error in the earlier measurements.

Data in Figures 2 and 3 leave little doubt that diffusion from apatite scales with grain radius, in a manner consistent with correspondence between the diffusion domain and the physical grain; this is contrary to earlier conclusions based on limited lower-quality data [*Wolf et al.*, 1996b]. Taking the highest-quality results (the 160–180 μm fractions in Figure 1), and assuming a mean radius for these grains of 85 μm, yields $D_0 \sim 50$ cm^2/s. This value is intermediate to the D_0 values obtained from the geometrically better controlled "resurfaced" slabs, which give values of 130 and 8 cm^2/s for c-parallel and c-perpendicular diffusion, respectively.

Because diffusivity scales with grain size, the closure temperature must scale similarly. Extrapolation of the diffusivities measured on the oriented sections indicates that c-perpendicular and c-parallel diffusion coefficients are within a factor of 2 of each other over the temperature range of partial helium retention (75–45°C) [*Wolf et al.*, 1998]. Coupled with the elongated c axis of most apatite grains (e.g., most length/diameter ratios in granitic apatites studied in detail were in the range 2–4 [*Wolf et al.*, 1996a]), c-perpendicular diffusion should control helium loss from apatite. Therefore the most appropriate geometry for modeling He diffusion from apatite and for calculation of closure temperatures is an infinite cylinder, although the results obtained from this geometry are indistinguishable from those obtained assuming plane sheet or spherical geometry.

An important implication of correspondence between the physical grain and the diffusion domain is that the He concentration profile at the edge of the grain is controlled not only by diffusion but by ejection of high-energy α particles. The effect of α ejection is to produce a rounded concentration profile across the outermost ~15 μm of the crystal [*Farley et al.*, 1996]. As a result, the He concentration gradient driving He diffusion from the grains will be less steep than it otherwise would be. A numerical model for an apatite cooling at a constant rate [*Wolf et al.*, 1998] that incorporates this effect indicates a modest increase in the closure temperature of ~2°C relative to that computed ignoring this phenomenon using *Dodson*'s [1973] method. Figure 7 shows the closure temperature for Durango apatite computed as a function of grain size and cooling rate

and including the increase predicted from α ejection rounding. Over 2000 apatite grains analyzed for He age at Caltech yield a roughly Gaussian distribution with a mean cylinder radius (half of the distance across the hexagonal prism) of 60 ± 20 μm (1σ). This then implies a best estimate for the closure temperature of typical apatites with the diffusion characteristics of Durango apatite of about 66°C assuming 10°C/Myr cooling rate. This value is lower than previous estimates based primarily on Durango apatite because the earlier experiments were done on large grains [*Wolf et al.*, 1996a]. In practice, the grain sizes are determined routinely for correction of α ejection [*Farley et al.*, 1996], so making adjustment for this effect when interpreting helium ages is straightforward and requires little additional work.

A related effect arises from attempts to measure diffusion coefficients of samples which have not had the surface removed prior to diffusion coefficient measurement. This effect is particularly significant in the first few percent of helium yield where the common assumption of a homogeneous concentration profile is seriously in error because of ejection. For these steps the apparent diffusivities will be lower than the true diffusivity. As the fraction of gas removed increases, the significance of the boundary condition is reduced, and measured diffusivities will rise toward the true diffusivity [*Fechtig and Kalbitzer*, 1966]. Note that this effect only applies to intact whole crystals; e.g., crystals that are fractured (like the Durango grains studied here) will have surfaces with concentration gradients unaffected by ejection that will reduce or eliminate the effect. If not taken into account, the result may be an overestimation of the helium retentivity of the apatite, the degree of which depends upon the heating schedule and fraction of gas released. From a practical perspective, there are two ways to deal with this phenomenon when measuring diffusion coefficients. The first is to extract a substantial fraction of the total helium from the sample prior to measuring diffusion coefficients, thereby minimizing the effects of the initial concentration profile. This approach is complicated by the fact that the rate of helium release at a given temperature drops rapidly with the cumulative fraction of helium released, so long-duration steps may be required. Furthermore, the steps designed to "strip" this initial condition must be conducted at temperatures below the irreversible transition in diffusion behavior, at about 265°C in Durango. Alternatively, the outermost surfaces can be removed, or the crystals fractured, so as to expose an unrounded concentration profile. Removing of surfaces or fracturing of grains will change the diffusion domain size, so this must be taken into account when estimating the closure temperature of the sample. In addition, as shown by the experiments on the polished slabs, care must be taken to ensure that removal of surfaces has not modified diffusivity. In either case a cycled heating schedule is critical because it can show conclusively whether the diffusion coefficients measured at a given temperature are stable and independent of the fraction of helium remaining in the sample.

A final complication of the correspondence between physical grain size and diffusion domain is that different parts of a crystal have different effective ages depending upon how close they are to the surface of the grain. As a consequence, the measured age of a crystal fragment may be substantially different from the true age of the entire crystal. In the case of titanite this effect is serious because only rarely can a whole euhedral grain be analyzed [*Reiners and Farley*, 1999]. Fortunately, this effect is not particularly serious for apatite because grains very commonly are euhedral, or at least are prismatic fragments that will retain a representative sampling of the age distribution within the crystal.

4.2. High-Temperature Behavior and Possible Explanations

Two phenomena observed in these experiments are not consistent with simple thermally activated volume diffusion: the irreversible change in diffusion parameters that occurs as apatite is heated above 265°C, and the transient high diffusivity that occurs in low-temperature steps immediately following a much higher-temperature step. The data in Figure 5 indicate that as Durango apatite is heated above ~265°C, the activation energy and D_0/a^2 decrease systematically until about 400°C. This change in diffusion characteristics is the cause of the downward curvature of diffusion arrays above ~300°C noted by previous workers [*Zeitler et al.*, 1987; *Wolf et al.*, 1996b]. This transition is independent of the fraction of gas extracted and so cannot be attributed to the presence of multiple diffusion domains or sites with differing diffusion parameters. Possible explanations for the transition include structural and/or compositional modifications, and annealing of defects. A comparison of the X-ray diffraction pattern of unheated Durango grains with that from grains heated above 400°C reveals no structural change. Similarly, differential thermal analysis and thermogravimetry provide no support for any change in crystal structure or composition through this temperature range (K. A. Farley, unpublished data, 1999).

A possible role for structural defects in controlling noble gas diffusion has been suggested by many previous workers [e.g., *Lee*, 1995, and references therein; *Trull et al.*, 1991; *Wolf et al.*, 1996b]. This possibility is strongly supported by the present data: the temperature of the transition in diffusion behavior coincides with rapid annealing of fission tracks (Figure 6), a reasonable proxy for defect annealing. Specifically, when held for 1 hour (comparable to the holding time for the diffusion experiments), fission tracks in Durango apatite begin to shorten at ~280°C and are completely gone by 370°C [*Green et al.*, 1986]. This suggests that the two phenomena are related in some way. *Lee* [1995] investigated noble gas diffusion behavior involving coupled volume diffusion and "short-circuit" diffusion through crystal defects. Although *Lee* [1995] found that a variety of behaviors are possible within such a coupled system, none of these behaviors are similar to that observed for He in apatite. Most notably, *Lee* [1995] modeled defects as fast pathways for diffusion, yet the correspondence between defect annealing and enhanced He diffusivity in apatite suggests instead that defects act to slow diffusive loss (at least at temperatures <265°C).

Defects might impede diffusion in several ways. For example, it is possible that He release in a defect-free crystal occurs via diffusion through channels. Such channels may be blocked by extended defects such as stacking faults, planar defects, screw dislocations or radiation damage, causing an alternative (lattice?) pathway to dominate He release in defect-rich crystals. Thus the systematic modification of diffusion behavior between 265 and 400°C might indicate progressive creation of throughgoing channels as defects anneal. A comparison to the data in Figures 5 and 6 can be used to estimate the diffusion parameters for hypothetical "channel" and "lattice" mechanisms. Specifically, prior to annealing that ensures above 265°C the lattice mechanism governs He loss from Durango apatite. This mechanism has been well documented by the experiments presented here and has $E_a \sim 32$ kcal/mol. As annealing be-

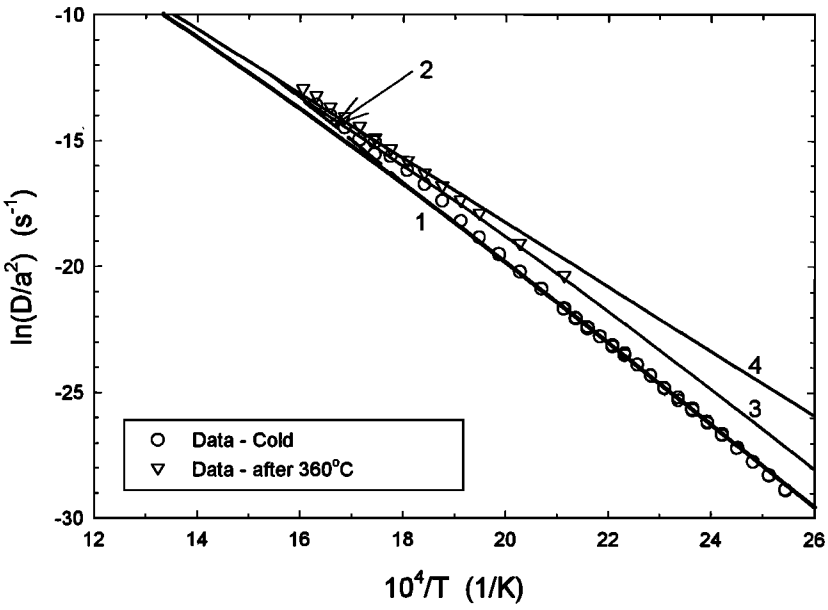

Figure 8. Helium-trapping model for the effects of defects on helium release from apatite. Symbols are the diffusivity data plotted in Figure 5. Lines are the computed diffusivities assuming that a temperature-dependent fraction of the He is immobilized in defects, according to (5), modified by the degree of defect annealing: 1, no annealing; 2, "in situ" annealing; 3, preannealed at 360°C; 4, total preannealing. The in situ annealing curve matches the diffusivity data obtained on a Durango sample experiencing a monotonically increasing heating schedule starting at low T. Curve 3 matches the Durango data obtained after initial heating of the sample to 360°C.

gins, this mechanism is shut-down, and the alternative "channel" mechanism begins to dominate. For the multipath diffusion that occurs while both mechanisms are active, the bulk diffusivity is the diffusivity of the individual mechanisms weighted by the fraction of He atoms in each pathway provided local equilibrium exists between the two (see *Lee* [1995] for a detailed discussion of multipath diffusion). After total annealing (grains heated above 400°C), the "channel mechanism" governs He loss, with a much lower activation energy of ~24 kcal/mol. While this model provides a straightforward (if ad hoc) explanation for the transition in diffusion behavior, it provides no obvious explanation for the transient high diffusivity after cooling from elevated temperatures (Figure 6).

Trull et al. [1991] proposed an alternative possibility: crystal defects may act as traps for helium, immobilizing some fraction of it from diffusive migration. If there is an equilibrium between trapped He in defects and free helium (He_t and He_f, respectively):

$$He_f \rightarrow He_t \quad k_t = [He_t]/[He_f] \tag{1}$$

where k_t is the equilibrium constant, and if only He_f is free to diffuse, then the observed diffusivity will be lower than the diffusivity observed in a defect-free crystal (see *Crank* [1975] for derivation):

$$D_{obs} = D_{vol}/(k_t + 1) \tag{2}$$

Here obs denotes the observed and vol denotes the defect-free volume diffusivity. It is reasonable to assume that both the equilibrium between free and trapped helium and the volume diffusivity of the crystal obey Arrhenius relationships:

$$k_t = k_{t,0} \exp(-E_t/RT) \tag{3}$$

$$D_{vol}/a^2 = D_{vol,0}/a^2 \exp(-E_a/RT), \tag{4}$$

where E_t and E_a are the activation energies for trapping and volume diffusion and $K_{t,0}$ and $D_{vol,0}$ are the trapping and diffusivity at infinite temperature. Equation (2) then becomes

$$D_{obs}/a^2 = (D_{vol,0}/a^2) \exp(-E_a/RT)/[k_{t,0} \exp(-E_t/RT) + 1]. \tag{5}$$

The temperature dependence predicted by this equation can be divided into two regimes. At sufficiently low-temperatures the trapping term ($k_{t,0} \exp(-E_t/RT)$) will greatly exceed unity (i.e., most helium is trapped), such that (5) reduces to

$$D_{obs}/a^2 \sim (D_{vol,0}/a^2)(1/k_{t,0}) \exp[-(E_a - E_t)/RT]. \tag{6}$$

At the high-temperature extreme the trapping term will become negligible compared to unity, and (2) reduces to the volume diffusion expression:

$$D_{obs}/a^2 \sim (D_{vol,0}/a^2) \exp(-E_a/RT) \tag{7}$$

Diffusion coefficients complying with (6) and (7) will plot as separate straight lines on an Arrhenius plot. At temperatures intermediate between these extremes a transitional behavior will occur and will plot as a curved segment connecting the two linear regimes.

Figure 8 illustrates the behavior of (5) with E_a = 25.4 kcal/mol, E_t = −7.5 kcal/mol, $k_{t,0} = 2 \times 10^{-3}$, and $D_{vol,0}/a^2 = 1500$. With these parameters the model mimics the well-established position and curvature of the He diffusion Arrhenius plot but does not predict the irreversible change in diffusion characteristics starting at 265°C. However, as indicated by the fission track annealing experiments, defects and

thus presumably the He traps disappear in this temperature range. This effect can be incorporated into the model by reducing the equilibrium constant for trapping as damage anneals, for example, in proportion to the relative abundance of traps: $k_t^* = [\text{trap}]k_t$, where [trap] ranges from unity to zero as the damage is annealed. The fission track length measurements of *Green et al.* [1986] suggest that annealing of damage in apatite occurs in the temperature range 275–375°C. By assuming [trap] drops linearly from unity at 275°C to zero at 375°C, the diffusion curves in Figure 8 were produced. For a sample heated monotonically from low temperature the effect of annealing is minimal, just a slight deviation in the position of the transition ("in situ" annealing curve). This modified form of (5) fits the Durango data well when the sample experiences monotonically increasing temperatures. However, if the defects are annealed partially or completely prior to the diffusion measurement (for example, by heating above 265°C), the effects are more significant. A fan of curves increasingly rotated toward higher diffusivity at low temperature are produced as the degree of preannealing increases. This behavior is very similar to the rotation seen in Figures 5 and 6 and matches well the Durango data obtained after heating to 360°C. Ultimately, the pure volume diffusion array is obtained (equation (7)).

A final observation that can be qualitatively accommodated by this model is the transient behavior that occurs when measuring diffusivity at low temperatures after cooling from a higher temperature (Figure 6). This phenomenon occurs when the maximum temperature experienced by the sample is <400°C but disappears once the sample has been heated above this value (Figure 6). The transient behavior may be attributed to a kinetic control on the equilibrium between free and trapped helium. When the sample is heated to high temperatures, the fraction of free helium is increased according to (3). If equilibrium is not immediately restored when the sample is cooled back down, then according to (5) the low-temperature diffusivity will be higher than at equilibrium. The measured diffusivity would drop as equilibrium between free and trapped helium is achieved. The fact that this transient phenomenon disappears once the sample is heated above 400°C is consistent with the model because the traps are completely annealed above this temperature.

Regardless of model, a critical question for apatite helium thermochronometry is whether the total abundance of defects affects the helium retentivity in the low temperature regime and, if so, how and when the defects are acquired. If the abundance of radiation damage defects is important, then there may be a general correlation between He or fission track abundance and He retentivity, and He retentivity might be expected to increase with helium age. Similarly, it is possible that apatites varying in defect abundance might vary in He retentivity. Measurements of a single apatite alone cannot be used to test these predictions. This issue is considered in more detail in a companion paper exploring variations in diffusivity among a range of apatites (K. A. Farley, manuscript in preparation, 2000).

5. Conclusions

The key observations regarding He diffusion from Durango apatite are as follows:

1. At temperatures <265°C, He diffusion plots on an extremely linear Arrhenius array. Temperature cycling experiments confirm that He diffusivity is independent of cumulative fraction of gas released, indicating a single diffusion domain and Fickian mechanism. The activation energy for He release from Durango apatite is ~33 kcal/mol.

2. He diffusivity scales with the inverse square of the grain size, providing compelling evidence that the grain itself is the diffusion domain.

3. There is a suggestion of only weak anisotropy in He diffusion through apatite. At temperatures of interest for He retention in nature (45–75°C), diffusivity on the *c*-parallel and *c*-perpendicular axes differs by less than a factor of 2. Given the typical aspect ratio of the apatite hexagonal prism and the observation that diffusivity scales with the inverse square of the grain radius, diffusive loss from apatite will be controlled by losses in the *c*-perpendicular direction. The most appropriate geometry for modeling helium loss from apatite is an infinite cylinder, and a in D/a^2 can be approximated by the half width of the prism.

4. Taking all of these observation together, the best estimate for the helium closure temperature from Durango apatite of ~90 μm radius is 68°C assuming a cooling rate of 10°C/Myr. This value varies by ±5°C when grain radius varies from 50 to 150 μm. An important implication of correspondence between physical grain and diffusion domain is that the ejection of high-energy α particles from grain edges will round He concentration profiles more than diffusion alone would and hence will reduce the rate of helium loss. Modeling indicates that this effect is minor, equivalent to about a 2°C increase in closure temperature for typical cooling scenarios.

5. The high-temperature deviation from simple Arrhenius behavior noted by previous workers is a thermally induced phenomenon that begins at ~265°C and is apparently complete by ~410°C. It is irreversible; helium diffusivity permanently shifts to lower E_a and D_0/a^2 values once an apatite has experienced this temperature range.

6. The temperature window over which the transition in diffusion characteristics occurs coincides closely with that of fission track annealing. This suggests that the change in diffusion behavior reflects annealing of defects and/or radiation damage sites that act to impede He mobility. If so, the total abundance of defects or radiation damage may influence He diffusion. Further investigation of this question is necessary. As indicated by fission track annealing studies [*Green et al.*, 1986], the temperature of annealing varies with apatite chemical composition, so the temperature at which the transition in diffusivity occurs may vary with apatite composition.

7. The work presented here demonstrates that it is critical to perform diffusion experiments at temperatures lower than that at which diffusion behavior is irreversibly modified. In Durango apatite this occurs at ~265°C, but it may occur at lower temperatures in other apatites. Measurements made after an apatite has been heated above this transition temperature will yield anomalously low closure temperatures. In general, thermally cycled diffusion experiments must be used to establish whether and at what temperature this transition occurs in other apatites. Cycling experiments are also important for detecting and eliminating effects associated with apatite surfaces, such as anomalously rapid release from apatites with rough surfaces and slow release associated with rounding of the He concentration profile from sample preparation, α ejection, or the sample's thermal history.

Acknowledgments. I wish to thank G. Rossman for extensive discussions of apatite mineralogy and for assisting with the DTA and TG

measurements, and L. Hedges for sample preparation. This work was supported by the National Science Foundation.

References

Crank, J., *The Mathematics of Diffusion*, 414 pp., Oxford Univ. Press, New York, 1975.

Dodson, M. H., Closure temperatures in cooling geological and petrological systems, *Contrib. Mineral. Petrol.*, *40*, 259–274, 1973.

Farley, K. A., R. A. Wolf, and L. T. Silver, The effects of long α-stopping distances on (U-Th)/He ages, *Geochim. Cosmochim. Acta*, *60*, 4223–4229, 1996.

Farley, K. A., P. Reiners, and V. Nenow, An apparatus for high-precision helium diffusion measurements from minerals, *Anal. Chem.*, *71*, 2059–2061, 1999.

Farver, J., and B. Giletti, Oxygen and strontium diffusion kinetics and potential applications to thermal history determinations, *Geochim. Cosmochim. Acta*, *53*, 1621–1631, 1989.

Fechtig, H., and S. Kalbitzer, The diffusion of argon in potassium bearing solids, in *Potassium-Argon Dating*, compiled by O. A. Schaeffer and J. Zahringer, pp. 68–106, Springer-Verlag, New York, 1966.

Green, P., I. Duddy, A. Gleadow, P. Tingate, and G. Laslett, Thermal annealing of fission tracks in apatite, 1, A qualitative description, *Chem. Geol.*, *59*, 237–253, 1986.

House, M. A., B. P. Wernicke, and K. A. Farley, Dating topography of the Sierra Nevada, California, using apatite (U-Th)/He ages, *Nature*, *396*, 66–69, 1998.

Lee, J., Multipath diffusion in geochronology, *Contrib. Mineral. Petrol.*, *120*, 60–82, 1995.

Lippolt, H. J., M. Leitz, R. S. Wernicke, and B. Hagedorn, (U+Th)/He dating of apatite: Experience with samples from different geochemical environments, *Chem. Geol.*, *112*, 179–191, 1994.

Lovera, O., F. Richter, and T. Harrison, Diffusion domains determined by ^{39}Ar released during step heating, *J. Geophys. Res.*, *96*, 2057–2069, 1991.

McDowell, F., and R. Keizer, Timing of mid-Tertiary volcanism of the Sierra Madre Occidental between Durango City and Mazatlan, Mexico, *Geol. Soc. Am. Bull.*, *88*, 1479–1487, 1977.

Reiners, P., and K. A. Farley, Helium diffusion and thermochronometry of titanite, *Geochim. Cosmochim. Acta*, in press, 1999.

Trull, T. W., M. D. Kurz, and W. J. Jenkins, Diffusion of cosmogenic ^{3}He in olivine and quartz: Implications for surface exposure dating, *Earth Planet. Sci. Lett.*, *103*, 241–256, 1991.

Warnock, A. C., P. K. Zeitler, R. A. Wolf, and S. C. Bergman, An evaluation of low-temperature apatite U-Th/He thermochronometry, *Geochim. Cosmochim. Acta*, *61*, 5371–5377, 1997.

Wolf, R. W., K. A. Farley, and L. T. Silver, Assessment of (U-Th)/He thermochronometry: The low-temperature history of the San Jacinto Mountains, California, *Geology*, *25*, 65–68, 1996a.

Wolf, R. W., K. A. Farley, and L. T. Silver, Helium diffusion and low temperature thermochronometry of apatite, *Geochim. Cosmochim. Acta*, *60*, 4231–4240, 1996b.

Wolf, R. W., K. A. Farley, and D. Kass, A sensitivity analysis of the apatite (U-Th)/He thermochronometer, *Chem. Geol.*, *148*, 105–114, 1998.

Young, E., A. Myers, E. Munson, and N. Conklin, Mineralogy and geochemistry of fluorapatite from Cerro de Mercado, Durango, Mexico, *U.S. Geol. Surv. Prof. Pap.*, *650-D*, D84–D93, 1969.

Zeitler, P. K., A. L. Herczig, I. McDougall, and M. Honda, U-Th-He dating of apatite: A potential thermochronometer, *Geochim. Cosmochim. Acta*, *51*, 2865–2868, 1987.

K. A. Farley, Division of Geological and Planetary Sciences, California Institute of Technology, MS 170-25, Pasadena, CA 91125.

(Received June 29, 1999;
accepted September 30, 1999.)